Anal. Chem. **1998,** *70,* 4929−4938

Electrospray Ionization High-Resolution Ion Mobility Spectrometry−Mass Spectrometry

Ching Wu, William F. Siems, G. Reid Asbury, and Herbert H. Hill, Jr.*

Department of Chemistry, Washington State University, Pullman, Washington 99164-4630

A hybrid atmospheric pressure ion mobility spectrometer is described which exhibits resolving power approaching the diffusion limit for singly and multiply charged ions (over 200 for the most favorable case). Using an electrospray ionization source and a downstream quadrupole mass spectrometer with electron multiplier as detector, this ESI-IMS−MS instrument demonstrates the potential of IMS for rapid analytical separations with a resolving power similar to liquid chromatography. The first measurements of gas-phase mobility spectra of mass-identified multiply charged ions migrating at atmospheric pressure are reported. These spectra confirm that collision cross sections are strongly affected by charge state. Baseline separations of multiply charged states of cytochrome *c* and ubiquitin demonstrate the improved resolving power of this instrument compared with previous atmospheric pressure ion mobility spectrometers. The effects of electric potential, initial pulse duration, ion−molecule reactions, ion desolvation, Coulombic repulsion, electric field homogeneity, ion collection, and charge on the resolving power of this ion mobility spectrometer are discussed.

For more than twenty-five years, ion mobility spectrometry (IMS) has been used as a method for trace organic analysis, finding important application in the vapor-phase detection of explosives, drugs, and chemical warfare agents.[1] While the primary targets of IMS analysis have been volatile organic compounds using radioactive ionization, recent developments in electrospray ionization have enabled the analysis of nonvolatile organics from liquid-phase samples.

Electrospray as an ionization source for ion mobility spectrometry was first demonstrated by Dole and co-workers in 1972[2] by electrospraying lysozyme into an ion mobility spectrometer to produce three broad peaks. In Dole's instrument, the nitrogen drift gas was introduced into the spectrometer at the "rear of the spray tube" in order to help sweep ions downstream. As the drift gas flow was increased, more efficient evaporation of the solvent was observed and the lysozyme ions drifted faster. However, ion peaks resulting from these experiments were very broad and did not demonstrate the presence of multiple charges on the lysozyme. Later, Dole and co-workers reported work with polystyrene, speculating that the broad peaks were due to excess solvent ions, which were adsorbed to the surface of the macroion aggregates.[3] Finally, they concluded that because of the difficulty in evaporating the solvent from the electrosprayed ions under atmospheric conditions, electrospray ionization would be useful only for mass spectrometry in which the solvent could be efficiently eliminated under vacuum conditions.[4] Smith and co-workers also found that it was difficult to separate electrosprayed proteins by IMS due to inefficient desolvation of the electrosprayed droplets.[5] Their data resembled that of Dole's earlier work. Unlike Dole's arrangement, in which the gas flow was in the same direction as ion migration, we have reported the need for a counterflow of heated, dry nitrogen drift gas to efficiently evaporate the solvent from electrosprayed droplets.[6] This counterflow design produced stable and completely desolvated electrosprayed ions, exhibiting reduced mobility constants that were reproducible with respect to temperature, flow, and solvent type.[7] Application of electrospray ionization-ion mobility spectrometry (ESI-IMS) was demonstrated as a detection method for liquid chromatography,[8] capillary electrophoresis,[9] and liquid process streams.[10]

The difficulty with this initial counterflow ESI-IMS design was that the heated drift gas raised the temperature of the electrospray sufficiently to volatilize the solvent before it could exit the needle and generate the spray. Thus, to increase sensitivity and stability,[11] corona spray was often preferred over true electrospray conditions. To address this prespray solvent evaporation problem we developed a water-cooled electrospray ionization source that

* Corresponding author: (tel) (509) 335-5648; (e-mail) hhhill@wsu.edu.

(1) Eiceman, G. A.; Karpas, Z. *Ion Mobility Spectrometry*; CRC Press: Boca Raton, FL, 1994.

(2) Gieniec, M. L.; Cox, J., Jr.; Teer, D.; Dole, M. *20th Annual Conference on Mass Spectrometry and Allied Topics,* Dallas, TX, June 4−9, 1972.

(3) Dole, M.; Gupta, C. V.; Mack, L. L.; Nakamae, K. *Polym. Prepr. (Am. Chem. Soc., Div. Polym. Chem.)* **1977**, *18* (2), 188−193.

(4) Gieniec, J.; Mack, L. L.; Nakamae, K.; Gupta, C.; Kumar, V.; Dole, M. *Biomed. Mass Spectrom,* **1984**, *11* (6), 259.

(5) Smith, R. D.; Loo, J. A.; Ogorzalek, R. R.; Busman, M. *Mass Spectrom. Rev.* **1991**, *10*, 359−451.

(6) Shumate, C. B.; Hill, H. H., Jr. Northwest Regional ACS Meeting, Bellingham, WA, June 1987.

(7) Shumate, C. B. An *Electrospray Nebulization/Ionization Interface for Liquid Introduction into an Ion Mobility Spectrometer* Ph.D. Thesis, Washington State University, 1989.

(8) McMinn, D. G.; Kinzer, J. A.; Shumate, C. B.; Siems, W. F.; Hill, H. H., Jr. *J. Microcolumn Sep.* **1990**, *2*, 188−192.

(9) Hallen, R. W.; Shumate, C. B.; Siems, W. F.; Tsuda, T.; Hill, H. H., Jr.; *J. Chromatogr.* **1989**, *480*, 233−245.

(10) Shumate, C. B.; Hill, H. H., Jr. Electrospray Ion Mobility Spectrometry—Its Potential as a Liquid-Stream Process Sensor. In *Pollution Prevention in Industrial Processes—The Role of Process Analytical Chemistry*; Breen, J. J., Dellarco, M. J., Eds.; ACS Symposium Series 508; American Chemical Society: Washington, DC, 1992.

(11) Shumate, C. B.; Hill, H. H., Jr. *Anal. Chem.* **1989**, *61*, 601−606.

10.1021/ac980414z CCC: $15.00
Published on Web 10/24/1998

could be interfaced directly to high-temperature IMS.[12] The advantages of this cooled electrospray source included rapid desolvation of sprayed droplets, prevention of solute precipitation in the spray needle, efficient transmission of ion spray into the IMS, and elimination of corona ionization.[13] In addition, both signal/noise (S/N) ratio and resolving power were improved for ESI-IMS by using the Fourier transform mode of operation.[14] With the cooled electrospray source, IMS proved to be a sensitive and practical detection method for liquid chromatography with detection limits as low as 1×10^{-15} mol s^{-1} and a linear response range of 3−4 orders of magnitude.[15]

While the development of electrospray ionization expanded the domain of IMS into polar and nonvolatile compounds, the low resolving power of ion mobility spectrometry has continued to limit the analytical potential of IMS as a separation device. Resolving power has been investigated throughout the history of analytical IMS,[16−26] with definitions of resolving power based on mass separation,[17] separation of pairs of peaks,[18] or a single-peak-based quotient.[19] The now generally accepted single-peak-based measurement of IMS resolving power is

$$R = t_d/w \tag{1}$$

where t_d is the ion drift time and w is the ion pulse duration at the detector measured at half of the maximal intensity. The first atmospheric pressure ion mobility spectrum, reported in 1970 for dimethyl sulfoxide, showed a resolving power of 30 [20] by this definition. Since that time, all commercial atmospheric pressure ion mobility spectrometers have had similar resolving power, despite theoretical predictions of higher values.

Revercomb and Mason[16] described four phenomena affecting ion pulse characteristics measured at the detector: (1) the initial ion pulse width and shape introduced into the drift region, (2) broadening by mutual Coulomb repulsion between the ions, (3) broadening by diffusion as the ion pulse drifts down the electric field, and (4) ion−molecule reactions with the drift gas or with impurities. They used the Einstein relation between the diffusion coefficient, D (in $cm^2\ s^{-1}$), and the mobility, K (in $cm^2\ V^{-1}\ s^{-1}$)

$$D = kTK/ez \tag{2}$$

and developed an expression for measured pulse width in cases where Coulombic repulsion and ion−molecule reactions are unimportant and where the initial ion pulse has a Gaussian shape of duration t_g at half-maximum

$$w^2 = {t_g}^2 + \left(\frac{16kT \ln 2}{Vez}\right){t_d}^2 \tag{3}$$

where k is Boltzman's constant, T is the temperature of the drift gas in kelvin, V is the potential across the drift length, e is the elementary charge, and z is the number of charges on the ion. In the limit, as t_d becomes very large compared to t_g, the *diffusion-limited resolving power* is obtained from eq 3

$$R_d \equiv \lim R\left(\frac{t_g}{t_d} \to 0\right) = \left(\frac{Vez}{16kT \ln 2}\right)^{1/2} = 0.300\left(\frac{Vez}{kT}\right)^{1/2} \tag{4}$$

For typical IMS devices and conditions (10 cm drift tube with a 300 V cm^{-1} electric field, 125 °C temperature), R_d is on the order of 100 for singly charged ions, but this limit has been elusive.

Spangler and Collins[17] obtained good qualitative agreement to experimental IMS peak shapes by convoluting a step function representing initial pulse shape with a Gaussian function representing diffusion. These authors also estimated that mutual repulsion has a small but measurable effect on pulse width, with this Coulombic broadening increasing as the initial pulse width increases. It should be noted that this result assumed the $\sim 1 \times 10^{-9}$ A total ion current typical of β^- emitter ion sources. Despite a good qualitative picture of peak shape, Spangler and Collins needed to introduce a "Townsend energy factor", $\eta = 2.7$, as a multiplier for the kT in the numerator of eq 3 in order to match experimental peak widths. Although this factor was rationalized as accounting for higher effective temperature of ions which are continually receiving energy from the electric field, the Townsend energy factor is known to be close to 1 for ions under atmospheric pressure IMS conditions.[24]

Siems et al.[24] have fit experimental pulse width data for singly charged ions in a number of IMS instruments to a semiempirical model based on eq 3

$$w^2 = \gamma + \beta {t_g}^2 + \alpha(T{t_d}^2/V) \tag{5}$$

and compared best-fit α, β, and γ parameters to the theoretical predictions $\gamma = 0\ s^2$, $\beta = 1$, and $\alpha = 9.57 \times 10^{-4}$ V/K (this α should be divided by $z^{1/2}$ for multiply charged ions). All three parameters were found to be greater than the theoretical predictions for each of the instruments studied. That α values were generally in the range $(1.2-1.5) \times 10^{-3}$ V/K, which was attributed mainly to electric field inhomogeneity, while β values of 1.1−1.3 were attributed to Coulomb repulsion, and γ values of $(0.5-2) \times 10^{-8}\ s^2$ were attributed to collector and amplifier rise time.

According to eqs 3 and 4, the primary ways to increase resolving power are to (1) raise the total voltage across the drift space, (2) decrease the initial pulse width, (3) lower the temperature of the drift gas, and (4) increase the number of charges on

(12) Wittmer, D.; Chen, Y. H.; Luckenbill, B. K.; Hill, H. H., Jr. *Anal. Chem.* **1994**, *66*, 2348−2355.
(13) Chen, Y. H.; Hill, H. H., Jr.; Wittmer, D. P. *Intl. J. Mass Spectrosc. Ion Processes* **1996**, *154*, 1−13.
(14) Chen, Y. H.; Siems, W. F.; Hill, H. H., Jr. *Anal. Chim. Acta* **1996**, *334*, 75−84.
(15) Chen, Y. H.; Hill, H. H., Jr.; Wittmer, D. P.; *J. Microcolumn Sep.* **1994**, *6*, 515−524.
(16) Revercomb, H. E.; Mason, E. A. *Anal. Chem.* **1975**, *47*, 970−983.
(17) Spangler, G. E.; Collins, C. I. *Anal. Chem.* **1975**, *47*, 403−407.
(18) Karasek, F. W.; Kim, S. H. Final Report, Contract 8SU77-00227; University of Waterloo Research Institute, Waterloo, Ontario, Canada, 1980.
(19) Rokushika, S.; Hatano, H.; Baim, M. A.; Hill, H. H. *Anal. Chem.* **1985**, *57*, 1902−1907.
(20) Cohen, M. J.; Karasek, F. W. *J. Chromatogr. Sci.* **1970**, *8*, 330−337.
(21) Mason, E. A. Ion Mobility: Its Role in Plasma Chromatography. In *Plasma Chromatography*; Carr, T. W., Ed.; Plenum Press: New York, 1984.
(22) Brokenshire, J. L. FACSS Meeting, Anaheim, CA, October 1991.
(23) Eiceman, G. A.; Karpas, Z. *Ion Mobility Spectrometry*; CRC Press: Boca Raton, FL, 1994; pp 99−100.
(24) Siems, W. F.; Wu, C.; Tarver, E. E.; Hill, H. H.; Larsen, P. R.; McMinn, D. G. *Anal. Chem.* **1994**, *66*, 4195−4201.
(25) Leonhardt, J. W.; Rohrbeck, W.; Bensch, H. Fourth International IMS Workshop, Cambridge, U.K., 1995.
(26) Dugourd, Ph.; Hudgins, R. R.; Clemmer, D. E.; Jarrold, M. F. *Rev. Sci. Instrum.* **1997**, *68*, 1122−1129.

the ions. To these primary factors we may add secondary factors suggested by eq 5—(5) increase the homogeneity of the electric field experienced by the ions, (6) decrease Coulombic repulsion within the ion pulse, and (7) shorten the rise time of ion collection and amplification. Finally we must recognize that higher resolving power will be achieved if we (8) study ions of high charge and/or low mobility (long t_d means resolving power close to the diffusion limit of eq 4), and (9) eliminate or mask the effects of labile clusters and ion—molecule reactions in the drift tube.

Several investigators have increased IMS resolving power by lengthening the drift tube along with increasing its voltage.[22−26] There are several reasons why increasing R by increasing voltage also requires making the tube longer. First, increasing V without increasing L also raises electric field strength, $E = V/L$, eventually resulting in electrical breakdown. Second, it has generally been deemed important to operate in the low-field regime in which the ion velocity remains proportional to E. This requires that IMS experiments be performed with an E/N ratio no more than (1−2) $\times$ 10^{-17} V cm^2 ,[21] where N is the number density of the drift gas (in cm^{-3}). Thus, for atmospheric pressure conditions, where $N = 2.46 \times 10^{19}$cm^{-3} (25 °C and 1 atm), the typical E values have been between 246 and 493 V/cm. Third, and with even more serious consequences for resolving power, increasing V without lengthening the drift tube also increases the relative contribution of t_g to w, since t_d decreases linearly with V. This means that, for a drift tube of given length, for each choice of t_g there is an optimum drift voltage, V_{opt}, that maximizes R[17,24]

$$V_{opt} = \left(\frac{\alpha T L^2}{2(\gamma + \beta t_g^2)^{1/2} K^2}\right)^{1/3} \qquad (6)$$

although for singly charged ions it is usually necessary to operate above V_{opt} to maintain signal strength.

Brokenshire constructed a 44-cm-long drift tube with a 10-cm diameter and reported a 5−10-fold increase in resolving power over traditional IMS instruments.[22] In Brokenshire's design, the aperture grid and the collector plate had a large diameter so that radial diffusion of ions did not decrease signal intensity.[23] We reported an IMS design in which the resolving power was improved over commercial instruments using a drift length of 15.6 cm and a drift voltage of 7000 V.[24] Leowhardt et al. have reported the use of drift fields up to 700 V/cm to reach R values as high as 120 for singly charged species.[25] Dugrourd et al. recently reported a low-pressure high-resolution IMS instrument where they place a potential of 14 000 V across a 63-cm drift tube at 500 Torr to produce a resolving power of 172.[26]

Watts and Widers[27] evaluated several ion mobility instruments with respect to resolving power. They calculated that the maximum resolving power (R_m) for the advanced vapor monitor (AVM) instrument (Graseby Dynamics, Ltd., Watford, Herts, WD25JX, U.K.) was 50. For the PCP instrument (PCP, 2155 Indian Road, West Palm Beach, FL), they calculated a range of maximum resolution from 50 to over 100 and a laboratory-constructed high-resolution tube (HRT) that was 44 cm in length had a theoretical maximum R between 125 and 275. Unfortunately, none of these instruments performed near their theoretical maximum. They suggested that Coulombic repulsion was the primary reason for low resolution in IMS but were unable to demonstrate this effect experimentally.

We report here the construction and evaluation of an atmospheric pressure ion mobility spectrometer with an electrospray ionization source and a quadrupole mass spectrometer to identify and detect those ions after mobility separation. Our experimental conditions give some a priori expectations about resolving power for this instrument. The relatively long drift times and multiple charges of ESI generated ions should tend to give relatively narrow peaks and larger R values. On the other hand, our high operating temperature, dictated by the need to desolvate ions, tends to lower R. In addition, we must watch for greater Coulomb broadening with the high total ion currents of ESI compared to β^- sources.

EXPERIMENTAL SECTION

Instrumentation. The electrospray ionization ion mobility/mass spectrometer instrument used in this study was constructed at Washington State University. A scale drawing of the instrument is shown in Figure 1. The water-cooled electrospray source was developed here several years ago.[12] In this ESI source, a water-cooled jacket surrounds the spray needle assembly and water-cooled nitrogen flows along the axis of and in contact with the spray needle. The nitrogen exits the spray assembly concentric with the needle and contributes to nebulization of the electrosprayed mist. The objective of cooling the spray needle and spray thoroughly is to prevent the heated drift gas from causing solvent evaporation inside the needle. A detailed drawing of this electrospray ionization source can be found on page 2350 in Figure 3 of ref 12.

The electrospray is drawn by electric potential toward and through a 16-mesh stainless steel focus screen into the desolvation region of the spectrometer, where the charged mist migrates in an electric field through a counterflow of heated nitrogen drift gas. During the few milliseconds of migration through the desolvation region, solvent evaporates from the droplets, leaving solvent and analyte ions. The temperature of the desolvation region can be controlled independently from the drift region by the introduction of a separately heated diluent drift gas at the interface between the desolvation region and the ion drift region. The temperature of the diluent drift gas can be selected to either cool or heat the drift gas as it passes into the desolvation region. In the experiments reported here, however, no diluent gas was added and the temperature in the desolvation region was the same as that in the drift region.

Two ion gates are located at the entrance and exit of the drift region of the spectrometer. These identical Bradbury−Nielsen-type gates are constructed using parallel Alloy 46 (California Fine Wire Co., Grover Beach, CA) wires 76 μm in diameter with a 0.64-mm spacing. The gates are "closed" by applying ±37.5 V to adjacent wires so that a ~1000 V/cm closing field is placed orthogonal to the drift field of the spectrometer. As positive ions approach the gate, they are collected on the negative wires of the gate, preventing them from passing through the gate. When the gates are "open", all gate wires are pulsed to a single voltage appropriate to the gate's position in the drift electric field.

Both the desolvation and drift regions are constructed of electrically conducting stainless steel and electrically insulating

(27) Watts, P.; Wilders, A. *Int. J. Mass Spectrom. Ion Processes* **1992**, *112*, 179.

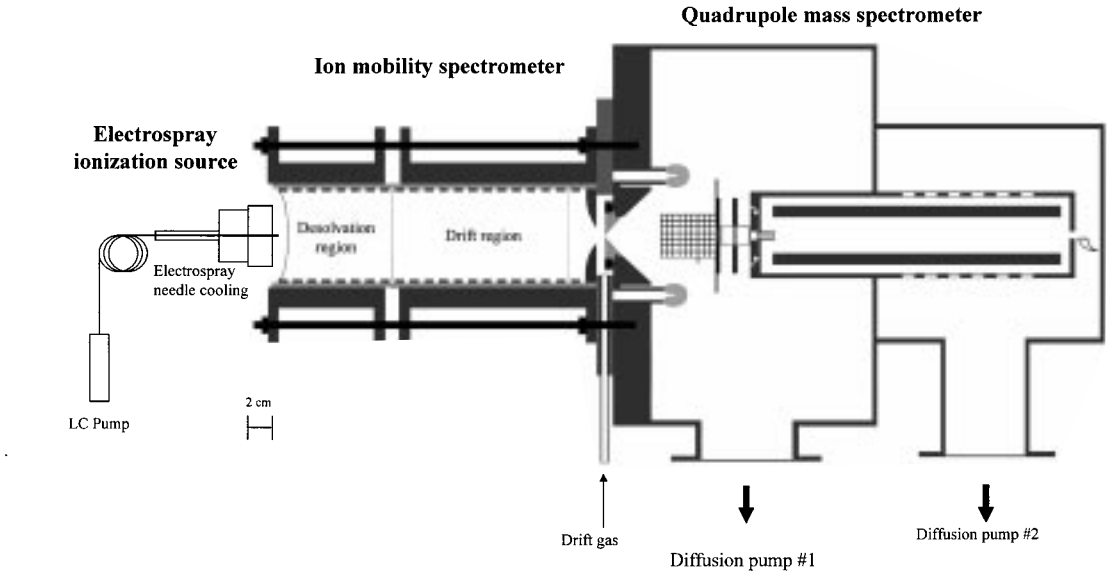

Figure 1. Instrument schematic of high-resolution ion mobility spectrometer with electrospray ionization and mass identification.

alumina rings stacked in an alternating and interlocking design. Each repeating unit of the tube, consisting of one conducting and one insulating ring, is 0.9 cm in length. The conducting rings are 0.8 cm wide, and the insulating rings 0.1 cm wide. The conducting rings are connected to one another via a series of 1-MΩ resistors. The dimensions of the rings are machined to be 4.9-cm i.d. and 5.7-cm o.d. The desolvation region is 7.2 cm in length, and the drift region is 13 cm in length.

A crucial portion of our apparatus is the interface between the ion mobility spectrometer and the mass spectrometer. It includes (1) the extraction region, (2) the extraction plate, (3) the buffer gas region, (4) the pinhole leak and the (5) adiabatic expansion region. The extraction region is the space between the ion exit gate and the pinhole through which the ions continue to migrate at atmospheric pressure (in an electrical field slightly higher than the drift field). The extraction plate is the tapering terminal ring of the mobility spectrometer beyond which only ions from the central 1.4 cm of the ion disk are permitted to continue toward the pinhole leak. The buffer gas region is the space between the extraction plate and the pinhole leak through which the drift gas is introduced. One intention of this arrangement is to disrupt the diffusion layer around the pinhole leak and to keep the leak clean and free from clogging. The 40-μm-diameter pinhole serves as the barrier between the atmospheric pressure of the drift tube and the vacuum of the mass spectrometer, while allowing a narrow ion beam to enter. Beyond the pinhole is the adiabatic expansion region where excess drift gas is pumped away and a sufficient electric field is maintained on the ions to prevent clustering or fragmentation. From the adiabatic expansion region, the ions are first drawn into a space bounded by a cylindrical screen and then focused through an einzel lens system into a quadrupole mass filter.

As shown on Figure 1, a metal carrier for the pinhole leak of the interface is mounted on a 16-cm-o.d. flange using a custom design metal−glass seal (fabricated from two standard metal−glass seals by Larson Electronic Glass, Redwood City, CA). This metal−glass seal serves as an expansion joint for the varying temperature gradient between the drift tube and the rest of the apparatus and allows us to vary the electrical potential on the pinhole. The pinhole leak is attached to the carrier by six 4/40 screws and a gold seal. The leak was fabricated by machining a central hole almost through a piece of 304 stainless steel, leaving a metal membrane 250 μm in thickness through which a 40-μm-diameter hole was drilled with a laser. The pinhole exhibited a leak flow rate of 28 cm^3/s at 15 psi. This flow rate brings us close to the maximum pumping capacity of our diffusion pumps. The vacuum chamber for the mass spectrometer was constructed at WSU and consisted of two chambers for differential pumping. Two Diffstak 160/700 diffusion pumps (Edwards High Vacuum Inc., 3279, Grand Island Blvd. Grand Island, NY) were mounted close to the upper chamber in order to achieve the maximum pumping capacity. Two ion gauges (Granville-Phillips, model 274006, Boulder, CO) were installed on the internal and external chamber for pressure measurements.

The mass spectrometer was a C50-Q (ABB Extrel, 575 Epsilion, Pittsburgh, PA) consisting of an API lens system designed by Extrel, a quadrupole mass filter with 0.95-cm-diameter rods 20 cm in length, and an electron multiplier (model 051-72) and preamplifier equipped with current amplification and ion-counting capability. The maximum m/z for our rods and power supply was 800. For these studies, the stock preamplifier was replaced with a Keithley 427 amplifier (Keithley Instruments, Cleveland, OH) and the amplified signal sent to the data acquisition system, which was constructed at WSU. A detailed description of the IMS control and data acquisition system can be found in ref 12.

General Operating Conditions. The electrospray ionization source was normally operated with a potential difference of 4000 V between the needle tip and the focus screen. The focus screen served to define the initial potential of the ion mobility desolvation region and drift tube. The potential on the screen was normally 5500 V while the potential on the spray needle was 9500 V. Samples were normally introduced into the spray needle with a solvent system composed of 47.5% water, 47.5% methanol, and 5% acetic acid. The solvent flow through the needle was controlled at 5 μL/min. The cooling water and gas flows were 55 and 630 mL/min, respectively, and were held at 19 and 25 °C, respectively.

Table 1. Operating Conditions

drift gas flow rate	800 mL/min (N_2)
sample flow rate	5 μL/min (CH_3OH:H_2O:CH_3-COOH = 47.5:47.5:5)
electrospray potential	9500 V
focus screen potential	5500 V
desolvation field	280 V/cm
drift field	280 V/cm
reference potential for ion entrance gate	3625 V
entrance gate closure potential	±37 V
reference potential for ion exit gate	628 V
exit gate closure potential	±28 V
extraction plate potential	251 V
pinhole leak potential	7.9 V
ion optics potentials	7.9, −4.9, −20.1, −7.4, −99.9, −23.2 V
internal chamber pressure	1.5×10^{-5} Torr
external chamber pressure	2.2×10^{-4} Torr

The electric field was maintained at 280 V/cm throughout the desolvation region and the ion drift region. A counterflow of heated, dry nitrogen drift gas was introduced between the extraction plate and the pinhole leak. This drift gas was preheated and introduced at a flow rate of 800 mL/min. In these experiments, no diluent gas for the desolvation region was introduced. The drift gas was normally heated to 250 °C and the drift tube pressure was at ~700 Torr measured for each individual experiment.

The ion optics of the MS system consisted of six elements with potentials of +7.9 (pinhole), −4.9 (screen), −20.1 (first element of einzel), −7.4 (second element of einzel), −99.9 (third element of einzel), and −23.2 (ELFS plate) V in order of the ion migration direction. The 1.2-MHz quadrupole mass filter was biased at −5.2 V. The electron multiplier was operated at potential of 1.75 kV, and the collision dynode at −4 kV.

These and other operating conditions are summarized in Table 1. Unless specified otherwise, the conditions listed in this table were used for all experiments described in this paper.

Test Compounds. Peptides and proteins (Sigma, St. Louis, MO) were used in this study without further purification and were dissolved in electrospray solvents with concentrations in the 10^{-5} to 10^{-4} M range. The solvent methanol, water, and acetic acid were HPLC grade reagents (J. T. Baker, Phillipsburg, NJ). Morphine standard in methanol (Supelco Inc., Bellefonte, PA) was diluted with mobile phase as needed.

RESULTS AND DISCUSSION

Figure 2 shows the relation between drift time and 1/V for doubly and triply charged positive ions of bradykinin, with drift voltages in the range 2307−3625 V. The solid lines are linear least-squares fits to the experimental data. In these plots, the slope of the line is the ratio of the drift length squared to the ion mobility, and the intercept measures the time an ion spends traveling from the pinhole at the end of the drift region to the particle multiplier. For both doubly and triply charged ions, the intercept is close to zero, indicating that the time for ions to drift through the adiabatic expansion region and mass analyzer is negligible compared to drift time under our operating conditions. A similar result was reported in previous IMS−MS experiments.[1] In addition, the linearity of the plots indicates both ions had well-defined mobilities when they traveled through the drift region, confirming that the desolvation process was complete before the ions exited the desolvation region.

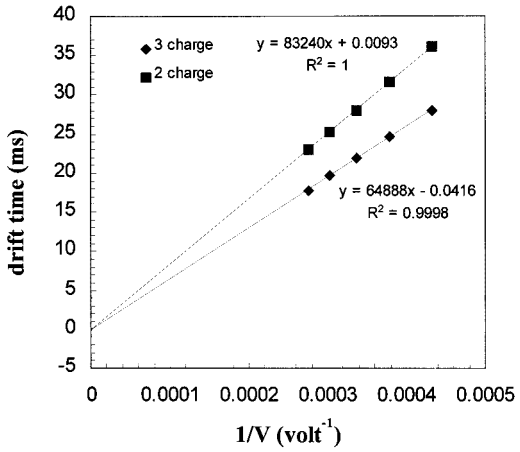

Figure 2. Drift time as a function of inverse drift voltage. Drift time was measured on ion mobility spectra of doubly and triply charged bradykinin ions created by electrospray ionization.

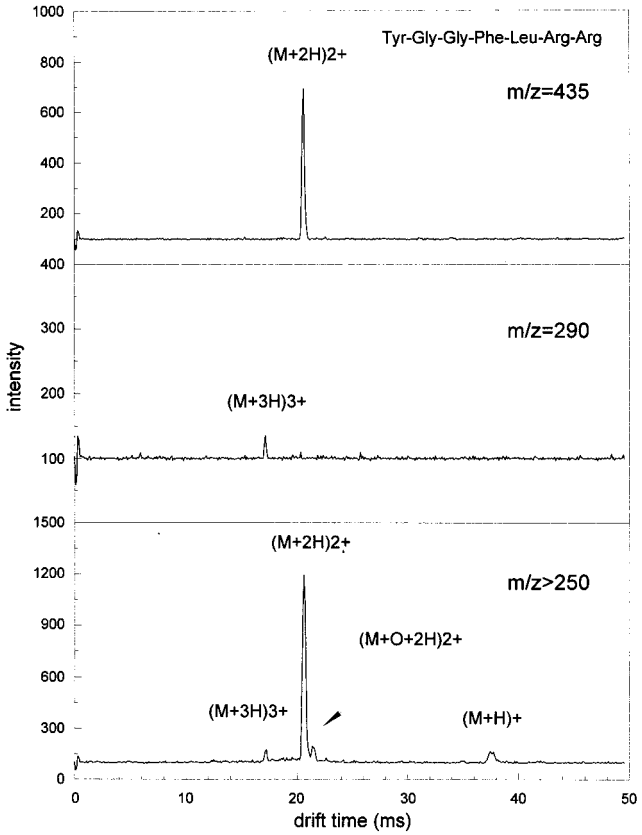

Figure 3. Ion mobility spectrum of dynorphin a fragment 1−7 with mass-identified ions.

Figure 3 shows data typical of the ESI-IMS−MS instrument constructed for this project. The three spectra in this figure were produced from electrospray ionization of the peptide dynorphin A 1−7 (MW = 867). The lower tracing is an ion mobility spectrum of all ions produced in the electrospray process with a molecular mass larger than 250 Da. This spectrum was obtained by pulsing the entrance gate open for 0.2 ms at a frequency of 20 Hz, holding the exit gate of the ion mobility spectrometer open

Table 2. Drift Time and Peak Width Data for Dynorphin A Using $t_g = 0.2$ ms

ion charge	t_d (ms)	w (ms)	R	R_d (calc)
+1	37.5	0.66	57	85
+2	20.5	0.29	71	120
+3	17.3	0.22	78	147

continuously, and using the mass spectrometer as a high-pass filter so that only ions with a mass greater than 250 Da would be detected by the electron multiplier. Under these conditions, ions with an m/z greater than 800 can be detected, even though the mass identification range of the quadrupole used in these experiments was limited to 800 Da.

The peak at 37.5 ms is thought to be the singly protonated peptide $(M + H)^+$ with $m/z = 868$, although this ion could not be mass identified due to the 800-Da limit of our quadrupole. Mass identification of the doubly and triply charged ion species, however, was possible. The middle tracing in Figure 3 was obtained by setting the mass spectrometer to pass $m/z = 290$, while the ion mobility spectrometer operated in the same manner used for the lower tracing. The single peak with a drift time of 17.3 ms matches the peak of highest mobility in the nonselective spectrum shown in the lower tracing and is believed to be the triply protonated peptide $(M + 3H)^{3+}$ with $m/z = (867 + 3)/3 = 290$. Similarly, the upper tracing in Figure 3 was obtained by setting the mass spectrometer to pass $m/z = 435$. The single peak at 20.5 ms corresponds to the most intense peak in the lower trace and is identified as a doubly protonated peptide $(M + 2H)^{2+}$ with $m/z = (867 + 2)/2 = 434.5$. This is the first time multiply charged ions have been mass identified for atmospheric pressure ion mobility spectrometry.

Drift time and peak width data for the +1, +2, and +3 peptide ions of Figure 3 are summarized in Table 2. If all three peptides had the same collision cross section, then the ratio of drift times for the +1/+2, +1/+3, and +2/+3 species would be 2, 3, and 1.5, respectively. That the measured ratios are 1.8, 2.1, and 1.2, respectively, indicates that the collision cross section increases as protons are added to the peptide, with a particularly striking increase as a third proton is added to the $(M + 2H)^{2+}$ species. Perhaps this is due to a strong repulsion of charges located on the two terminal arginine residues.

The measured resolving power of the ion mobility spectrometer for the three peptide ions (see Table 2) is quite striking and entirely typical of what we observe with this apparatus. Generally speaking, this device shows resolving power of ~2× or better, compared to what we have come to expect for IMS instruments of similar dimensions and operating conditions. For comparison, Table 2 shows R_d, the diffusion-limited maximum resolving power, predicted from eq 4 for these three peptide ions. As we discuss further below, for very narrow initial pulse widths we have frequently measured R values greater than R_d. We do not take this to mean that we have defeated diffusion, but rather to indicate that the actual resolving power of this device is close enough to the theoretical limit that the noise statistics of our measurements yield results above the maximum with fairly high frequency.

A practical consequence of increased resolving power is the ability to separate closely spaced peaks, such as the two peaks with drift times of 20.5 and 21.2 ms shown in the lower trace of Figure 3. The smaller of these two peaks was found to have $m/z = 443$, 8 Da greater than the m/z 435 measured for the larger $(M + 2H)^{2+}$ peak. The mass identifications confirm that these really are two different species, with mobilities differing by ~3%, that have been near baseline resolved by this IMS instrument, a condition we have never been able to achieve before with similar drift tubes. Incidentally, from the separation of these two peaks it might be reasoned that the mass dispersion of the IMS is 0.6 ms/8 Da = 0.08 ms/Da. The corresponding width in daltons for the peak at 20.5 ms would be (20.5 ms)/(57 × 0.08 ms/Da) = 4.5 Da, and the resolving power from the 20.5-ms peak calculated on a mass basis would be 435/4.5 = 97. The fact that this "mass" resolving power and the mobility resolving power do not agree is another reminder that mass and mobility cannot be directly compared. Because ion mobility separations are based on the size and shape of ions, rather than mass (mass is important only in that it changes the size of the ion), it is clearly absurd to measure the resolving power of an ion mobility spectrometer in terms of mass.

The identities assigned to these two ions were $(M + 2H)^{2+}$ for the peak at 20.5 ms as discussed above and $(M + O + 2H)^{2+}$ for the peak at 21.2 ms. The assignment of an oxygen adduct to an electrosprayed ion is reasonable and has been noted previously.[28] One explanation for the presence of $(M + O + nH)^{n+}$ ions when proteins or peptides are electrosprayed into mass spectrometers is that a corona discharge is present at the electrospray emitter tip. Alternatively, species may be oxidized in solution by electrolysis in the electrospray needle. Through variation of solvent flow and emitter tip potential, it may be possible to eliminate the formation of this adduct and/or to elucidate its formation mechanism.

To systematically examine the resolving power of the ESI-IMS−MS system, a number of interrelated factors must be considered: initial pulse width, electric field homogeneity, ion detection, Coulombic repulsion, ion statistics, ion−molecule reactions, ion desolvation and temperature, analyte concentration, and ionic charge.

Initial Pulse Width. Other than diffusion, the single most important contributor to IMS peak width is the initial width of the pulse. It is also the least interesting, as we know from the beginning how we must handle it: for highest possible R, use the lowest possible t_g that produces a sufficiently strong signal. Decreases of S/N with decreasing pulse width were observed. When initial pulse widths less than 0.05 ms were used, the signal became too weak to detect. This cutoff probably occurs because 0.05 ms is about the time required for an ion to pass completely through the region where the gate closure field significantly perturbs the drift field.

To understand the improved resolving power of the present ESI-IMS−MS, we want to remove the effects of the initial pulse width and consider the remaining "impulse response" of the IMS to an infinitely narrow initial ion pulse. Data to accomplish this are summarized in Table 3. It contains four studies of peak width for the $(MH)^+$ ion for two different concentrations of histidine (1 and 0.1 mg/mL), measured by either nonselective monitoring

(28) Morand, K.; Talbo, G.; Mann, M. *Rapid Comm. Mass Spectrom.* **1993**, *7*, 738.

Table 3. Histidine $(M + H)^+$ Peak Width Measured by Selected Ion Monitoring (SIM) and Nonselective Monitoring (NS) as a Function of Applied Pulse Width

C (mg/mL)	mode	t_g (ms)	t_d (ms)	$w \pm \sigma$ (ms)	$R \pm \sigma$	$(w^2 - t_g^2)^{1/2}$	w_d (ms)	β
1.0	NS	0.05	13.65	0.193 ± 0.037	71 ± 14	0.19	0.20	1.18
		0.10	13.63	0.242 ± 0.006	56 ± 1	0.22		
		0.20	13.61	0.304 ± 0.011	45 ± 2	0.23		
		0.40	13.71	0.479 ± 0.022	29 ± 1	0.26		
1.0	SIM	0.05	13.67	0.188 ± 0.026	73 ± 11	0.18	0.16	1.49
		0.10	13.62	0.217 ± 0.026	63 ± 8	0.19		
		0.20	13.61	0.276 ± 0.008	49 ± 1	0.19		
		0.40	13.64	0.516 ± 0.027	26 ± 1	0.33		
0.1	NS	0.05	13.76	0.151 ± 0.012	91 ± 7	0.14	0.14	1.37
		0.10	13.74	0.184 ± 0.019	75 ± 7	0.16		
		0.20	13.70	0.274 ± 0.014	50 ± 3	0.19		
		0.40	13.74	0.489 ± 0.013	28 ± 1	0.28		
0.1	SIM	0.05	*a*	*a*	*a*	*a*	0.11	1.39
		0.10	13.77	0.144 ± 0.013	96 ± 9	0.10		
		0.20	13.69	0.271 ± 0.017	50 ± 3	0.18		
		0.40	13.79	0.483 ± 0.056	29 ± 3	0.27		

[a] Signal too weak to measure.

(m/z >150, NS) or selective monitoring of the molecular ion (m/z = 156, SIM). For each of four t_g values, quadruplicate measurements of w yielded an average width and standard deviation. Although it is tempting to use eq 2 and subtract the effect of the initial width from the measured width to get a "diffusion-only" width, $(w^2 - t_g^2)^{1/2}$, this approach fails since $(w^2 - t_g^2)^{1/2}$ varies with t_g (see Table 3).

One reason for the dependence of $(w^2 - t_g^2)^{1/2}$ on t_g is that the initial pulse is not Gaussian in shape and its width depends on ion distribution across a closed gate. Although, of course, the electronic timing of the signal applied to the gate is known, the temporal profile of the ion pulse admitted to the drift tube is greatly influenced by the details of the interaction between the ion stream and the physical components of the gate. The ion stream is depleted of ions immediately upstream of the gate due to the action of the closure field (the "gate depletion" effect), and this disruption extends about as far upstream in the drift tube as the separation distance of the gate wires. A similar effect of closing the gate reduces ion density in the trailing edges of ion pulses admitted to the drift tube. The actual magnitude and spatial profile of this depletion will be different for ions of different mobility. Another contributor to our uncertainty about peak shape is Coulombic repulsion, which broadens the initial pulse to an extent that increases with ion density, mobility, and applied initial pulse width.

Because of these effects, we cannot know the true initial pulse width, and the best approach is to plot w^2 vs t_g^2 for several values of t_g.[24] Extrapolation of the nearly linear plot to $t_g^2 = 0$ yields the diffusion-only width, w_d, as the square root of the y intercept. This extrapolation eliminates not only the pulse width but also the effects of mutual Coulombic repulsion. In fact, the slope of the plot (the β of eq 5) is a measure of broadening due to Coulombic repulsion. This linear regression was performed for each of the sets of data in Table 3. The w_d and β values are given in the table.

The values of w_d given in Table 3 should be compared with the diffusion-limited peak width of 0.16 ms calculated from eq 4 for an ion of drift time 13.75 ms. We appear to be seeing essentially ideal diffusion-limited behavior from this IMS device when the effects of initial pulse width and Coulombic repulsion are removed. In terms of the analysis of eq 4 and ref 24 for this IMS essentially $\gamma = 0$ s^2 and α=1.0 × 10^{-3} V/K. If ref 24 was correct in concluding that the α values of the real IMS devices studied were 20−50% higher than ideal because of electric field inhomogeneity, we must conclude that the ESI-IMS−MS of this study has a nearly perfectly homogeneous electric field. Similarly if γ values greater than zero can be accounted for by slow collector and amplifier rise times in the devices studied in ref 24 then the present device must be faster in its response.

Electric Field Homogeneity. Past attempts to the create homogeneous drift fields have included increasing the diameter of the drift tube, increasing the number of drift rings per unit distance, and coating the inside of the tube with a resistive paint, creating a continuous voltage gradient. None of these approaches have resulted in high-resolution ion mobility spectrometry. In the present ESI-IMS−MS device, it seems clear that the ions contributing to the observed spectra experience not necessarily an electric field of superior homogeneity but what is just as good for maintaining narrow peaks: they experience nearly the *same* electric field. Only those ions which pass through the 40-μm-pinhole contribute to the signal, and if the trajectories of these ions are traced backward to their points of origin in the plane of the gate, we would find that ~67% of them come from an ~1.5-mm-diameter circle at the center of the gate. This follows because an initially infinitely thin disk of ions that spends 13.7 ms drifting through a 13-cm drift tube, diffusing to become a plug with temporal width of 0.16 ms at half-maximum, has a spatial thickness of 0.16 ms(13 cm/13.7 ms) = 0.15 cm. Since the ions have nearly the same transverse diffusion coefficient as longitudinal, the origins of the ions passing through the 0.040-mm pinhole, of negligible size compared to the 1.5-mm diffusion width, would be described as a Gaussian distribution of width 1.5 mm at half-maximum in the plane of the gate. Having a small plug of ions that travels through a narrow corridor in the most homogeneous central part of the electric field to reach the pinhole and contribute to our signal should be contrasted to ordinary circumstances in

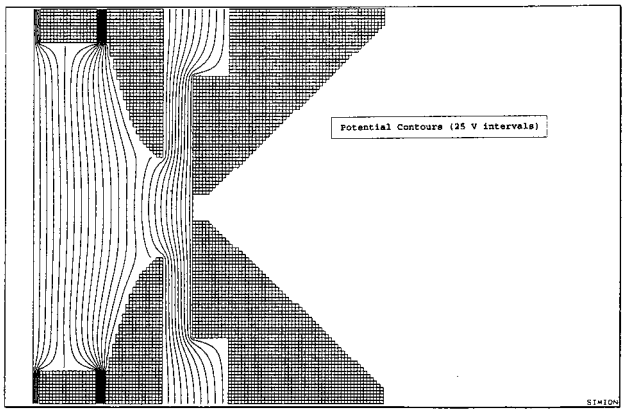

Figure 4. Simion plot of ion drift tube−mass spectrometer interface. Potential contour interval is 25 V. The distance between last electrode to pinhole inlet was 3 mm.

which an ion pulse nearly as wide as the drift tube is gathered on a collector of similar width. This is probably the main source of improvement in our resolution compared to ordinary IMS.

Ion Detection. People have used a direct pinhole interface between IMS and MS for years without noting resolving power as high as ours,[29] and one wonders at the reason for this. It is certainly not a result of our electrospray ion source. It may be that the electronics of earlier systems have simply been too slow to observe improved resolution. It may also be that highly attractive potentials used to increase the number of ions drawn through the pinhole have distorted and broadened the ion pulse. Our design keeps the equipotentials fairly flat right up to the pinhole, as may be seen in Figure 4.

On the related matter of our apparatus having a γ close to 0, this is certainly not the result of amplifier characteristics since the ESI-IMS−MS uses the same type of amplifier (with a 0.1-ms 10−90% rise time) that has been used for all our applications in recent years. However, our design does eliminate the aperture grid. Traditionally, IMS detection has been accomplished with a Faraday plate shielded by an open wire structure called an aperture grid located 0.5−1 mm ahead of the plate. Without the aperture grid, an ion pulse approaching the collector plate induces a current well before the pulse actually reaches the plate, broadening peaks significantly. The aperture grid shields the collector electrode from the incoming ion packet. To minimize pulse broadening, the distance between the aperture grid and collector should be as small as possible while the field between the two is as large as possible without distorting the drift field. Unfortunately, the shorter the distance between the grid and the collector or the larger the potential difference between the grid and the collector, the more sensitive is the collector to vibrational variations in the grid−collector distance. These variations lead to increased baseline noise in the detector. Thus, a compromise of conditions between those that produce acceptable baseline noise and those that produce acceptable pulse broadening is required, and in the optimum case, the inductive response of the collector probably begins ∼0.1 ms ahead of the arrival of the ion packet. In the present design, the need for an aperture grid is eliminated since the ions are detected by the electron multiplier of the mass spectrometer. This change may be the source of improvement in γ.

Coulombic Repulsion. The average β (= 1.36) for the four sets of experiments summarized in Table 3 is somewhat higher than the 1.1−1.3 range from ref 24. This may be the result of increased Coulombic broadening due to the higher ion currents of our ESI source compared to the ^{63}Ni sources of the reference. It is then somewhat surprising that the 1.0 mg/mL experiments have an average $\beta = 1.34$, nearly the same as the $\beta = 1.38$ of the lower concentration 0.1 mg/mL experiments. This lack of dependence of β on analyte concentration suggests that the additional broadening might be the result of higher concentration of solvent-derived ions, in which case the broadening would have to occur during the first few milliseconds after a pulse is admitted to the drift tube, before the solvent and analyte ions become separated. This situation could be clarified by a more exhaustive study with a wider range of concentrations.

Ion Statistics and Anomalously High Resolution. Table 3 contains two R values higher than R_d, and the w_d values for the 0.1 mg/mL samples are both below the 0.16-ms diffusion limit. While these results are statistically not exceedingly unlikely, and we certainly do not wish to challenge eq 2, we still have encountered anomalously high R values often enough with the ESI-IMS−MS apparatus, especially with low analyte concentration and/or low initial pulse widths, to spend some time trying to think of ways that falsely narrow peak widths could be obtained. The only possibility that has not been discarded as untenable is statistically inadequate sampling of the single ion pulses which comprise our signal.

A typical weak IMS pulse might consist of 10^4 ions ((10-pA peak current × 0.2-ms peak width)/1.6 × 10^{-19} C ion^{-1}), while it seems unlikely that the 40-μm pinhole has an ion-transfer efficiency greater than 10^{-5} (pinhole area/ion beam area ≅ (4 × 10^{-3}cm)^2/(1.25 cm)^2). Then the most intense IMS peaks (say 10^6 ions) will transfer ∼10 ions into the mass spectrometer, while the weakest peaks might produce one ion or less in 10 trials. Each ion striking the multiplier of the mass spectrometer produces a current spike containing ∼10^6 electrons and lasting a few tens of nanoseconds, and the amplifier with its 0.1-ms 10−90% rise time at 10^9V/A gain converts this spike into a ∼0.1 V pulse ∼0.2 ms wide. To measure peak widths correctly we must average enough of these single-ion pulses to adequately represent the ion spatial distribution in the IMS tube. It may be that for some weak signals we have used ion samples that are too small or rejected as "noisy" some of the outliers in our data and thereby underestimated the widths of these small peaks.

Ion−Molecule Reactions. The diffusion-limited peak widths in Table 3 are slightly narrower for the SIM data than for the corresponding nonselective data. Although one of our purposes in using a countercurrent flow of drift gas is to reduce penetration of the drift region by neutral molecules of sample and solvent, the wider peaks for the nonselective cases may be the result of ion−molecule reactions in the drift space. A neutral molecule, I, can react reversibly with an analyte M^+ to form an adduct or capture charge

$$M^+ + I \leftrightarrows MI^+ \quad \text{and/or} \quad M^+ + I \leftrightarrows M + I^+ \qquad (6)$$

If a peak composed mainly of M^+ also contains ions such as I^+

(29) Karpas, Z.; Stimac, R. M.; Rappoport, Z. *Int. J. Mass Spectrom. Ion Processes* **1988**, *83*, 163.

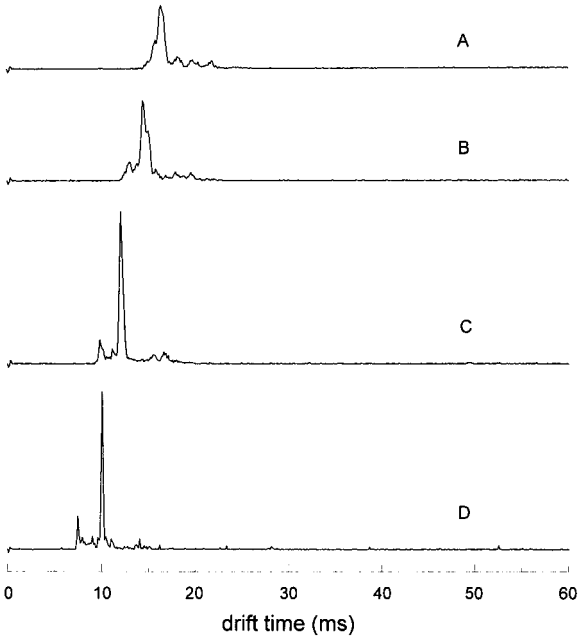

Figure 5. Ion mobility spectra of electrospray solvent under different temperatures: A, 100, B, 150, C, 200, D, 250 °C.

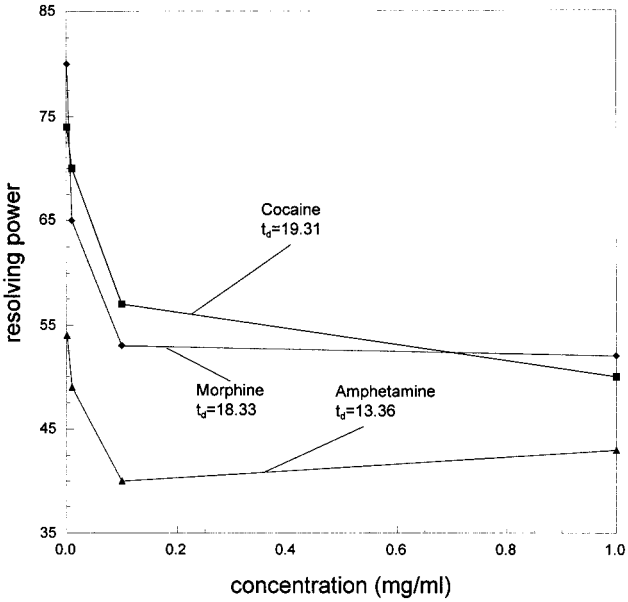

Figure 6. Measured ion mobility resolution of amphetamine, cocaine, and morphine under different sample concentration with mass selective detection: electrospray solvent, 49.5% water, 49.5% methanol, and 1% acetic acid.

and MI^+, having mobilities either less or greater than M^+, it is clear that the peak will be broadened relative to a peak composed of pure M^+. If the forward and reverse reactions of eq 6 are rapid relative to the mobility experiment, then selective detection will have no effect on peak width since the relative ionic composition will be uniform across the whole peak. However, if the reaction rates are on the same order as or slower than the mobility experiment, then the leading edge of the peak will accumulate ions more mobile than M^+ while the trailing edge will have a higher proportion of ions lower in mobility than M^+ in comparison to the central portion of the peak. In this case, mass selective detection will not record these ions in the leading and trailing edges of the peak, and the measured width will be less than with nonselective detection.

Desolvation and Temperature. According to eq 3, lowering the drift tube temperature is an effective means to increase the resolving power of an ion mobility spectrometer. On the other hand, we rely on the high temperature of the countercurrent drift gas to supply the heat needed to desolvate analyte ions, so it is important to operate our system at the lowest temperature that will accomplish this. Figure 5 compares ion mobility spectra of solvent ions obtained at four different temperatures. At 100 °C, poorly resolved peak clusters are observed at 16.6 (major), 18.2, 19.7, and 21.9 ms**.** As the drift gas temperature is increased to 250 °C, these peaks become better resolved and move to faster drift times, presumably as the number of clustered solvent ions decreases. In the 250 °C spectrum, the two major ions were mass identified as $m/z = 19$ (7.5 ms, H_3O^+) and = 75 (10.1 ms, $C_3H_7O_2^+$, protonated methyl acetate). As suggested by this study, we found that complete desolvation of analyte ions required a drift tube temperature of 250 °C.

Analyte Concentration. Note that the w_d values in Table 3 for the 1.0 mg/mL experiments are slightly greater than the corresponding values for the 0.1 mg/mL samples. Although it is tempting to attribute this observation to additional Coulombic repulsion with the greater ion density of the more concentrated samples, the coincidence of the β values argues against this. More extensive examination of this situation is needed. In a related study, Figure 6 shows resolution as a function of analyte concentration for cocaine, amphetamine and morphine with concentrations ranging from 1 to 1000 μg/mL. A constant t_g of 0.2 ms was used for these SIM measurements, and since lower concentrations of the sample produce a lower charge density in the migrating ion pulse, the low concentrations are expected to show higher resolving power if Coulombic repulsion is important. The figure shows this is indeed the case. The overall lower resolving power for amphetamine is probably the result of the shorter drift time for this analyte (13.36 ms vs 19.31 ms for cocaine and 18.33 ms for morphine), resulting in a greater relative contribution of t_g to the total peak width. For all three analytes, at concentrations less than 100 μg/mL resolution increases greatly, and in fact, for the lowest two concentrations of cocaine and morphine, R is above the diffusion limit. This rapid decrease in peak width at the lowest concentrations is contrary to what would be expected from Coulombic repulsion, since the repulsive force becomes less and approaches zero as the absolute charge density approaches zero. These low-concentration results are possibly due to inadequate sampling of the very weak signals, as discussed above. Whatever the explanation of these lowest concentration results, for best resolution it appears that the IMS should be operated at the lowest ion currents possible.

Ionic Charge. From eqs 3 and 4, we see that the diffusion-limited resolving power increases with the square root of the number of charges on the ion. Multiple charging of compounds by electrospray ionization is common, with 30 charges or more reported for some proteins. The combination of multiple charges and large collision cross sections with low analyte concentration and the other characteristics of our ESI-IMS−MS have acted in concert to produce the highly resolved ion spectra of two proteins, cytochrome *c* and ubiquitin, shown in Figure 7.

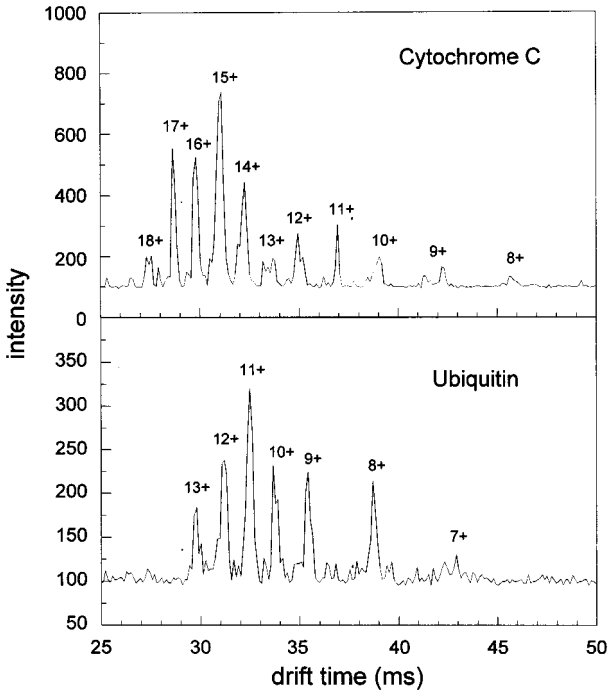

Figure 7. Ion mobility spectra of cytochrome *c* and ubiquitin—separation of multiply charged ions.

The numbers above each peak or peak cluster indicate the charge state of that peak or cluster. For example, the peak in the cytochrome *c* spectrum with a drift time of 28.7 ms was mass identified to be the $(M + 17H)^{17+}$ ion. The resolving power that was calculated from this ion was 120. The highest resolving power calculated from this spectrum was from the peak located at a drift time of 36.7 ms. Identified as the $(M + 11H)^{11+}$ ion, the resolving power was determined to be 216. Note the baseline separation of each charge state.

CONCLUSIONS

The improved resolving power exhibited by our ESI-IMS−MS appears to be due mainly to improved electric field homogeneity and detection speed, with contributions from selective ion monitoring and the tendency of target analytes appropriate for ESI to have long drift times and multicharged ions. For low concentrations and very narrow gate widths we have often noted anomalously high resolving power, possibly because of very small ion samples. We are certainly at the very limit of rise time possible with our electrometer amplifier and should probably change to time-to-digital conversion for these very weak signals.

There are two main avenues to further improve the resolving power of our apparatus. Operating the drift tube at much lower temperatures could greatly increase resolving power, although we would need to find another way to supply heat of vaporization directly to the ESI droplets. Second, resolving power could be increased by increasing the total drift voltage. As discussed in the introduction, to increase resolving power by increasing V it is also necessary to increase tube length to remain in the low-field regime.

In this connection it should be noted that Spangler has recently reported that, while ion velocity will no longer be proportional to the strength of the electric field, high-field conditions may further increase the resolving power of IMS.[30] Moreover, high-field conditions may vary the separation factor between ions. Separation factor α' is defined here for the ion mobility spectrometer in a manner similar to that used in chromatography:

$$\alpha' = K_1/K_2 = v_1/v_2 \qquad (7)$$

Where v_1 and K_1 are the ion velocity and mobility of the ion with the fastest drift time and v_2 and K_2 are the ion velocity and mobility of the ion with the longest drift time, respectively. For low-field conditions α' is constant, but for high-field conditions α' becomes a function of the electric field strength. While there has not been much published on ion mobility under high-field strength conditions, the transverse ion mobility spectrometer uses this phenomenon to maximize separation between two ions.[31] For time-of-flight IMS, however, more investigation is required to test the usefulness of high E fields for increasing resolution.

Ion mobility spectrometry, originally known as plasma chromatography and touted as a poor man's mass spectrometer, has, over the years, proved not to have sufficient resolving power to serve as a replacement for chromatography much less mass spectrometry. In fact, the resolving power of atmospheric pressure ion mobility spectrometers has been so low that IMS has primarily been useful only as a selective detection device after high-resolution chromatography. Thus, with the improvements in resolving power reported in this work, IMS appears poised to become a separation method in its on right, providing orthogonal separation data that complements rather than competes with those obtained with both chromatography and mass spectrometry.

ACKNOWLEDGMENT

The authors thank Dr. Glen Spangler for his initial advice in constructing the IMS−MS instrument and Dr. Gary Van Berkelfor discussions on the electrospray process. This project was supported in part by the Washington State University Drug Abuse Program, the Federal Aviation Administration Grant 97G009, and a Research Fellowship for C.W. provided by STEC, Inc., Japan. This paper was presented in part at the 45th ASMS Conference on Mass Spectrometry and Allied Topics, Palm Springs, CA, June 1997.

Received for review April 13, 1998. Accepted August 7, 1998.

AC980414Z

(30) Spangler, G. E. Fifth International IMS Workshop, Jackson, WY, **1996**.
(31) Buryakov, I. A.; Krylov, E. V.; Nazarov, E. G.; Rasulev, U. Kh. *Int. J. Mass Spectrom. Ion Processes* **1993**, *128*, 143.